Quantum dynamics in continuum for proton transport—Generalized correlation

Duan Chen[1,a)] and Guo-Wei Wei[2,b)]
[1]*Department of Mathematics, Michigan State University, East Lansing, Michigan 48824, USA*
[2]*Department of Electrical and Computer Engineering, Michigan State University, East Lansing, Michigan 48824, USA*

(Received 8 November 2011; accepted 14 March 2012; published online 5 April 2012)

As a key process of many biological reactions such as biological energy transduction or human sensory systems, proton transport has attracted much research attention in biological, biophysical, and mathematical fields. A quantum dynamics in continuum framework has been proposed to study proton permeation through membrane proteins in our earlier work and the present work focuses on the generalized correlation of protons with their environment. Being complementary to electrostatic potentials, generalized correlations consist of proton-proton, proton-ion, proton-protein, and proton-water interactions. In our approach, protons are treated as quantum particles while other components of generalized correlations are described classically and in different levels of approximations upon simulation feasibility and difficulty. Specifically, the membrane protein is modeled as a group of discrete atoms, while ion densities are approximated by Boltzmann distributions, and water molecules are represented as a dielectric continuum. These proton-environment interactions are formulated as convolutions between number densities of species and their corresponding interaction kernels, in which parameters are obtained from experimental data. In the present formulation, generalized correlations are important components in the total Hamiltonian of protons, and thus is seamlessly embedded in the multiscale/multiphysics total variational model of the system. It takes care of non-electrostatic interactions, including the finite size effect, the geometry confinement induced channel barriers, dehydration and hydrogen bond effects, etc. The variational principle or the Euler-Lagrange equation is utilized to minimize the total energy functional, which includes the total Hamiltonian of protons, and obtain a new version of generalized Laplace-Beltrami equation, generalized Poisson-Boltzmann equation and generalized Kohn-Sham equation. A set of numerical algorithms, such as the matched interface and boundary method, the Dirichlet to Neumann mapping, Gummel iteration, and Krylov space techniques, is employed to improve the accuracy, efficiency, and robustness of model simulations. Finally, comparisons between the present model predictions and experimental data of current-voltage curves, as well as current-concentration curves of the Gramicidin A channel, verify our new model. © *2012 American Institute of Physics*. [http://dx.doi.org/10.1063/1.3698598]

I. INTRODUCTION

Ion channels are fundamental components in various physiological processes, from cellular energy transduction, cardiac cycles, to human sensory systems. The importance of ion channels to biological science and biomedical engineering can never be overestimated. For instance, in human sensory systems, cooperations of sodium, potassium, and calcium channels, which are mediated by external stimuli (chemical, physical, mechanical, thermal, acoustic, or photonic ones, etc.), convert environmental signals, such as vision, hearing, somatic sensation (touch), taste and olfaction (smell), into electric signals recognizable by human brain. As a special type of ion permeation, proton transport plays a major role in energy transduction in a bioenergetic system. For example, chemical/biological energy is stored as proton gradients, then proton flux across cell membranes drives adenosine triphosphate generation in the mitochondria. Another important example of the function of proton channels occurs in the respiratory burst process of phagocytes such as human neutrophils. Due to these critical functions, ion channels have attracted a great deal of attentions in the past several decades, from experimental exploration,[1–3] theoretical investigation,[4–8] to numerical simulation,[9–13] modeling,[14–19] and mathematical analysis.[20–23] Generally, an ion channel system is extremely complicated, which consists of an ionic solvent, specific channel proteins and various lipid bilayers or cellular membranes.

The starting point to examine such a complex system is the solvation analysis, since almost all important biological processes in nature take place in aqueous environments. Solvent-solute interactions must be considered carefully. Additionally, the molecular structure of a channel protein is of

a)Present address: Mathematical Biosciences Institute, The Ohio State University, Jennings Hall 3rd Floor, 1735 Neil Ave., Columbus, Ohio 43210, USA.
b)Author to whom correspondence should be addressed. Electronic mail: wei@math.msu.edu.

paramount importance because it determines the gating mechanism, selectivity function, and the efficiency of the ion conductance of the channel in a complex environment. Apart from the molecular structure, dynamics of ion transport is another critical aspect. Regular ions may permeate membrane bilayers with the assistance of channel proteins via an electrohydro-diffusion mechanism, accompanying with the dehydration and rehydration processes, while proton transport also involves the hydrogen bond making and breaking process, which is often termed as Grotthuss mechanism.[24] In order to understand molecular mechanism of ion channel transport, it is indispensable to take into account molecular structures and dynamics.

Current major strategies for modeling general ion transport processes include molecular dynamics (MD), Brownian dynamics (BD), and the Poisson-Nernst-Planck (PNP) theory. MD is able to provide the most detailed descriptions in biomolecular systems and there are several user-friendly packages available, such as AMBER,[25] CHARMM,[26] or GROMOS,[27] etc. However, the use of MD in modeling the whole ion permeation process is still extremely computationally expensive, due to the long total simulation time needed to mimic the ion permeation time scale in large systems. It is instead utilized to estimate the mean-field potential and obtain necessary physical parameters such as diffusion coefficients of ions. Practically, BD and the PNP theory are powerful tools to study ion channels based on the mean-field approximation. Both the BD and PNP models have a number of similarities in their initial setups and computational approaches.[10,28,29] In the former approach, ions are treated as explicit particles, whereas in the PNP approach, all ions are further modeled by the continuum description through the electro-diffusion theory. Atomic details of the channel protein are retained in these two approaches to estimate electrostatic potentials, whose gradient drives the ion motion while details of water molecules are erased and treated as a dielectric continuum.

For Gramicidin A (GA) channel, the experimental data of voltage-current curves of proton transport[3] show much different characteristic from that of K^+ and Na^+ transport.[1] Diffusion models or Brownian dynamics may work well for describing the transport of heavy atoms or ions, but not for the transport of protons, which has to be treated quantum mechanically.[15,28,30–35] In view of transport mechanism, unlike other ions, protons transfer via the exchange of hydrogen nuclei along successive hydrogen-bond donors and acceptors, instead of via pure diffusion. Further, the hydrogen-bonded water chain (HBWC) may be compensated by some amino acid residues of the channel protein when the water molecules are not continuous in an extremely narrow channel pore.[36] In view of physical properties, proton has the lightest mass among all ions and an effective radius that is about 10^5 times smaller than other ions because it bears no electron. Proton transfer and all interactions with surrounding molecules are greatly facilitated by its light mass, tiny size, and thus, nuclear quantum effects (zero-point energy and quantum tunneling of hydrogen nuclei) are significant:[36,37] these unique characteristics are far beyond the description of simple diffusion models. There are many investigations of proton transport either in bulk water or transmembrane proteins in the literature. For example, dynamics of protons in bulk phase water are computed with an emphasis on a quantum dynamical treatment by Schmitt and Voth.[35] In an extensive effort, Roux and co-workers explored the single file of water molecules of the Gramicidin A channel and its ability to function as a proton wire via Feynman path integral dynamical simulations.[28,33,34] It is generally believed that nuclear quantum effects have a significant but no governing impact to proton transfer in equilibrium conditions.[28,33,34] However, under nonequilibrium initial conditions, such as the effect of an external electric field,[38] or a narrow situation in which hydrogen-bonding partners restricting the displacements of water molecules,[39] nuclear tunneling and nonadiabatic transitions may play an important role in the proton translocation.[28,37] In the past decade, handling nuclear quantum effects in proton transfer has become a standard practice in theoretical investigations. Yan *et al.* studied coherent proton transfer along HBWCs,[40] using the proton quantum dynamical approach developed by Cukier.[31,41] Recently, Shepherd and Morrison have reported the effects of different density functional theory (DFT) functionals to proton transfer through channel water-wires.[32] In fact, the use of quantum mechanical descriptions is a must when proton transfer or dislocation is coupled to electron transfer.[30,31,41,42] All these studies are based on a full-atom fashion.

Based on a general variational multiscale framework,[23] a series of differential geometry based multiscale models (DGMMs) have been established to study ion channels and proton transport.[16,17,19] A basic DGMM (Ref. 19) and a Poisson-Boltzmann-Nernst-Planck (PBNP) model[18] are proposed for regular ion channels. In a series efforts, a basic quantum dynamics in continuum (QDC) model[16] and its combination with variational solvent-solute interface (VSI) (Ref. 17) are introduced to model the proton transport through membrane proteins. These DGMMs follow the same spirit that they originate from the solvation analysis and the total energy functionals are constructed with multiscale, multiphysics, and multidomain descriptions on an equal footing. Furthermore, a set of matched interface boundary (MIB) based computational techniques[43–46] is employed to overcome related numerical challenges in realistic simulations.[13] These techniques provide rigorously second-order convergent solutions for complex geometries, nonsmooth interfaces, and singular charges of membrane channel proteins, therefore high accuracy and efficient of simulations are ensured.

In current ion channel models, most emphasizes are focused on the long-range force or electrostatic interactions between ions and surroundings. Explicit description of short-range interactions is often neglected and the corresponding effects are encapsulated in model parameters, such as diffusion coefficients or relaxation time of ions. While short-range interactions including dipolar, induced dipolar, quadrupolar, dispersion, or size effects are also important components for more detailed permeation dynamics such as ion selectivity. For example, because the ions of Na^+ and K^+ have the same charge, simple electrostatic potential landscape is not able to distinguish two species. One has to consider detailed ion-water interactions in order to explain the selectivity of

potassium channels. Many successful improvements, such as dielectric barrier and ionic size effects, have been developed in classical continuum models.[10,47–49] Under our QDC framework, this type of interactions is termed as generalized correlations (GCs) and must be modeled by quantum mechanical means, and more importantly, its ingredients are extended. The GC is of special importance to the proton transport process because of the Grotthuss (or hop-and-turn) mechanism.[32] The profiles of water molecules (for example, length and angle of hydrogen bond) in narrow channel pore are significantly different from those in bulk region. Protons experience dehydration and rehydration processes during the permeation. One of the GC interactions, the ion-water interaction, may contribute to the channel selectivity. Additionally, as mentioned above, protons are able to form and break hydrogen bonds with residues of channel protein as well. Therefore, the GC must contain interactions of proton with water, proton with channel, and proton with themselves and needs to be modeled quantum mechanically.

Short-range proton-environment interactions, especially proton-water interaction, have been intensively studied at atomic level. Both protons and water molecules are considered as individual atoms and the proton hop-turn mechanism is investigated in bulk water and in single-file water chain or "water wire." The existence of proton in the solvent can generally be represented either as a hydronium (H_3O^+) or as a "Zundel cation" ($H_5O_2^+$). In general, the translocation barrier of a proton depends strongly on the interatomic (proton-water and water-proton-water) distance and the orientation of water molecules, which are usually treated as control parameters in various models. It is widely believed that changes in the hydrogen-bond connectivity of water molecules (the length or angle of the hydrogen bonds) facilitate the process of proton translocation.[50] Based on these theories, a diversity of simulation methods has been proposed to model proton transport in water, focusing on different aspects. Examples include Car-Parrinello simulations of liquid water, *ab initio* calculations of protonated water clusters, path integral, centroid, classical molecular dynamics, Monte Carlo simulations using central force fields, and empirical valence bond methods which are used both as general methods and as *ad hoc* sets of functions and parameters. In these models, water molecules are described as individual atoms with SPC/E, TIP3P, or PM6 models. However, there is no best water model for all purposes, and one has to make a compromise between accuracy, number of predictable physical phenomena and computational expense. Quantum dynamics theory is also introduced to study the proton-water reaction. To reduce computational cost, it is nature to apply the quantum mechanics (QM) only to the proton and restrict the quantum subsystem to a Born-Oppenheimer plane, i.e., the environment is evolving according to classical MD. A mixed QM/MD simulation of proton transfer is proposed in Ref. 51 based on the GROMOS96e MD program. This model gives a detailed description of the coupling between the quantum mechanics of proton and the classical environment. Apart from the electrostatics energy, the proton potential energy of the Hamiltonian consists of proton-water pair interaction and water-proton-water triple interaction, whose shapes are both fitted to relaxed MP2/6-31G potential energy surfaces of the respective clusters *in vacuo*, based on the SPC/E water model. Pair particle interactions and their impact to the transport equations of density, velocity and energy were considered in the Boltzmann kinetic theory framework by Snider *et al.* in 1996.[52,53] Solution to the generalized Boltzmann equation and transport coefficient evaluation were also carried out.

The objective of the present work is to explore a quantitative formulation of the GC so as to improve our multiscale QDC model[16,17] for the prediction and analysis of proton transport across membrane proteins. The GC has been an important ingredient but treated less quantitatively in our earlier QDC models.[16,17] In this work, it will be modeled in a general formulation for short-range ion-ion, ion-water, and ion-protein interactions. Unlike other traditional models, including *ab initio* MD or hybrid ones on proton transport in solvent, in which water molecules are treated as explicit individuals, the water in our QDC models is considered as structureless continuum and described by a density function. In this setting, the present work provides an efficient way to embed quantum mechanical description of protons into the classical environment, which is mainly approximated as a continuum in order to balance the computational efficiency and physical complexity. A GC functional, depending on densities of water, proton, all other ion species and the membrane protein, is proposed and serves as part of potential energy in the Hamiltonian of protons. Therefore, the newly developed formulation can be easily adopted in our previous QDC theory. The total energy functional of the system consists of the proton energy and the solvation free energy of the membrane channel system. The proton energy is described by the quantum formalism and includes the kinetic and potential contributions. An interesting point is that, the potential energy of protons encompasses the GC and electrostatics as part of the system solvation energy. As a result, all the ingredients are fit into our multiscale/multiphysics/multidomain framework on an equal footing. By using the variational principle, we derive new governing equations, which are coupled and related to the GC formulation.

The rest of this paper is organized as follows. Section II is devoted to the theory of the QDC model and the formulation of generalized correlations. A general energy functional is constructed for the proton transport. The generalized correlation kernel is provided in the context of the proposed QDC formalism. In Sec. III, we derive a set of coupled governing equations by using the variational principle for the QDC description of the proton system. The solution procedure of this coupled equation system is discussed in detail. A number of mathematical algorithms, including the Dirichlet-to-Neumann mapping (DNM), the MIB method, and Krylov space techniques are utilized to implement the proposed model in a computationally efficient manner. The numerical results of the present formulation are given in Sec. IV. We first illustrate the effects of geometric constraints of a narrow channel to the generalized correlation and the channel Hamiltonian. Additionally, we utilize the Gramicidin A, to validate the present theory and model. Comparison is given to experimental measurements of proton transport. This paper ends with brief concluding remarks.

II. THEORY AND FORMULATION

To establish notation and facilitate further development, we first give a brief review of the theoretical formulation of the QDC model of the proton transport system. The quantitative description of the generalized correlation functional is presented.

A. Total free energy functional of the system

A proton transport system is extremely complicated in its biological structure, dynamics, and transport process. This system constitutes a bulk solvent, a channel pore, and molecule/membrane regions, which have distinguished physical and biological characteristics. In terms of materials with different levels of interests, there are protons, other mobile ions, water molecules, and membrane protein, etc. Figure 1 gives an illustration of the QDC model for a proton transport system. The system is restricted in a three-dimensional (3D) rectangular domain, with electrodes on two sides for the application of transmembrane voltages. There are at least two subdomains, the solvent domain Ω_s and the membrane/protein domain Ω_m, which are separated by the solute-solvent interface. In the multiscale treatment, the continuum approximation for the solvent and discrete atomic description for the membrane protein are implemented on the two subdomains, receptively. As indicated in Figure 1, the channel system is described by different physics and governing equations. These governing equations are derived from a total free energy functional which brings together multidomain, multiscale, and multiphysics in a unified fashion.[17]

$$
\begin{aligned}
G_{\text{Total}}[S,\Phi,n] = \int \Big\{ & \gamma|\nabla S(\mathbf{r})| + pS(\mathrm{r}) + \rho_0(1-S(\mathbf{r}))U_{ss} \\
& + S(\mathbf{r})\left[-\frac{\epsilon_m}{2}|\nabla\Phi|^2 + \Phi\rho_f\right] \\
& + (1-S(\mathbf{r}))\left[-\frac{\epsilon_s(\mathbf{r})}{2}|\nabla\Phi|^2 + \Phi n(\mathbf{r})q - k_BT\sum_j^{N_c'} n_j^0\left(e^{-\frac{q_j\Phi-\mu_j}{k_BT}}-1\right)\right] \\
& + (1-S(\mathbf{r}))\left[\int \frac{\hbar^2 e^{-(E-\mu_p)/k_BT}}{2m(\mathbf{r})}|\nabla\Psi_E(\mathbf{r})|^2 dE + U_{\text{GC}}[n] + U_{\text{Ext}}[n]\right] \\
& + (1-S(\mathbf{r}))\lambda\left[\frac{N_p}{V_\Omega} - \int e^{-\frac{E-\mu_p}{k_BT}}|\Psi_E(\mathbf{r})|^2 dE\right]\Big\} d\mathbf{r}. \qquad (1)
\end{aligned}
$$

The above functional depends on three major variables, the solute-solvent characteristics function $S(\mathbf{r}) : \mathbb{R}^3 \mapsto \mathbb{R}$, the electrostatic potential $\Phi(\mathbf{r}) : \mathbb{R}^3 \mapsto \mathbb{R}$, and the number density of ions of major interests (i.e., proton in this work) $n(\mathbf{r}) : \mathbb{R}^3 \mapsto \mathbb{R}$. The first line of the right-hand side of Eq. (1) gives the nonpolar solute-solvent interaction energy of the system in the form of molecular surface area, volume and solvent-solute dispersion interaction, where γ, p, ρ_0, and U_{ss} are the surface tension, hydrodynamic pressure, solvent density, and solute-solvent interaction potential, respectively. The second and third lines give the polar or electrostatic contribution to the system, with ϵ_m and $\epsilon_s(\mathbf{r})$ being dielectric constants of the biomolecular and solvent regions. The charge sources of the electrostatics come from the ions of interests, other mobile ions and fixed charge of the channel protein. The number density of proton $n(\mathbf{r})$ is obtained via quantum dynamics and q is the fundamental charge. All fixed charges of the channel protein are discretely represented by the charge density ρ_f. For other mobile ions, the Boltzmann distribution has been applied with k_B, T and μ_j being the Boltzmann constant, the temperature and the general electrochemical potential of jth ion species, respectively. Here, n_j^0, q_j, and N_c' are the reference number density, ionic valence of the jth ionic species, and the total number of other ionic species, respectively.

The proton is described in a quantum mechanical formulation in terms of kinetic and potential energies. Here $\hbar$ is the reduced Planck constant, and $m(\mathbf{r})$ is effective mass of the proton. The kinetic energy is represented by the

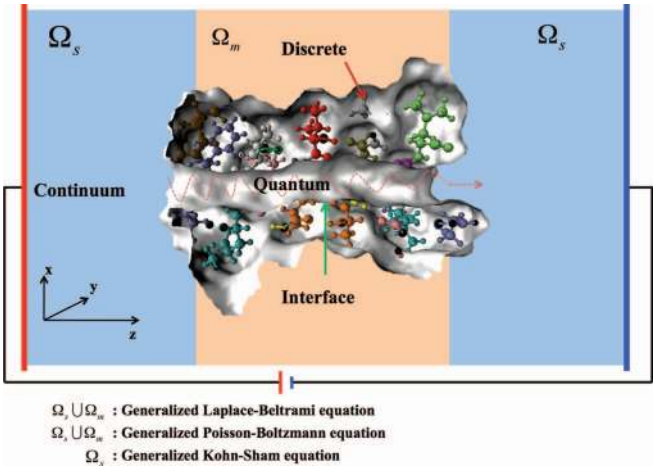

FIG. 1. Model illustration: the whole system is divided into two subdomains, the solvent domain Ω_s and membrane/channel domain Ω_s. Multiscale treatments and multiphysics descriptions are applied in corresponding subdomains and materials. The z-direction is considered as the proton transport direction. Profile of water in the channel pore is not displayed.

gradient of the proton wavefunction $\Psi_E(\mathbf{r})$. The potential energy of protons is approximated as functionals of the proton density. Here $U_{\mathrm{GC}}[n]$ and $U_{\mathrm{Ext}}[n]$ are the generalized correlation and external energies of protons, respectively. It should be pointed out that the electrostatic energy of protons has been accounted in the previous line, namely $\Phi n(\mathbf{r})q$. It was shown in our previous work[16] that a complete description of electrostatic source terms leads to a full prescription of the proton electrostatic potential energy.

Without protonation and deprotonation in the channel, proton transport over membrane protein pore can be modeled as a scattering problem and the corresponding Hamiltonian has an absolutely continuous spectrum. To compute the statistical rate of proton transport, we utilize the Boltzmann statistics to integrate the energy spectrum E. The wavefunction and number density of the proton have the following relation:

$$n(\mathbf{r}) = \int |\Psi_E(\mathbf{r})|^2 e^{-\frac{E-\mu_p}{k_B T}} dE, \tag{2}$$

where μ_p is the general electrochemical potential of protons. Finally, the additional term in the last row of Eq. (1) is a Lagrange multiplier for the constraint of the proton density due to the total number of protons N_p over the total volume $V_\Omega = \int_\Omega d\mathbf{r}$. When there are protonation and deprotonation in the channel protein, the present formulation has to be modified to account for reactive scattering processes. However, this aspect is not investigated in the present work.

The total energy functional (1) represents a multiphysical and multiscale framework that contains the continuum approximation for the solvent, while explicitly takes into account the channel protein in discrete atomic details. More importantly, it puts the classical theory of electrostatics and the quantum mechanical description of protons on an equal footing. Similar energy frameworks have been developed in our recent work for biomolecular systems[19,23,54] and nanoelectronic devices.[55]

B. Generalized correlation (GC)

The electrostatic potential plays a significant role in the proton transport. However, there are many other interactions that are also important for proton dynamics in the system. These additional interactions, termed as generalized correlation, include van der Waals interactions, dispersion interactions, proton-water dipolar interactions, proton-water cluster formation or dissociation, proton spin effects, proton-protein interaction, etc. For example, one of generalized correlation effects is an energy barrier to the ion transport due to the change in the solvation environment from the bulk water to a relatively dry channel pore, such as a single-file water chain. For proton transport, the energy needed to form and/or break the hydrogen bond depends on the proton-water distance and angles between hydrogen bonds, which are different in the channel and bulk conditions. As part of the generalized correlation, this type of proton-water interactions has been intensively studied in the literature.[32,35,50,51,56,57] Figure 2(a) provides a schematic diagram that illustrates a basic methodology. In this picture, the circles in various colors represent different atoms of a channel protein. Both the proton and water molecules are considered as individual particles. In such an explicit representation, the proton-water and water-proton-water configurations are parametrized by α, β, angles between the excess proton and two hydrogen atoms in the water molecule, as well as $\mathbf{r}$, the distance between oxygen atom and the excess proton. It is based on these quantities that the proton-water interaction mechanism is studied in different

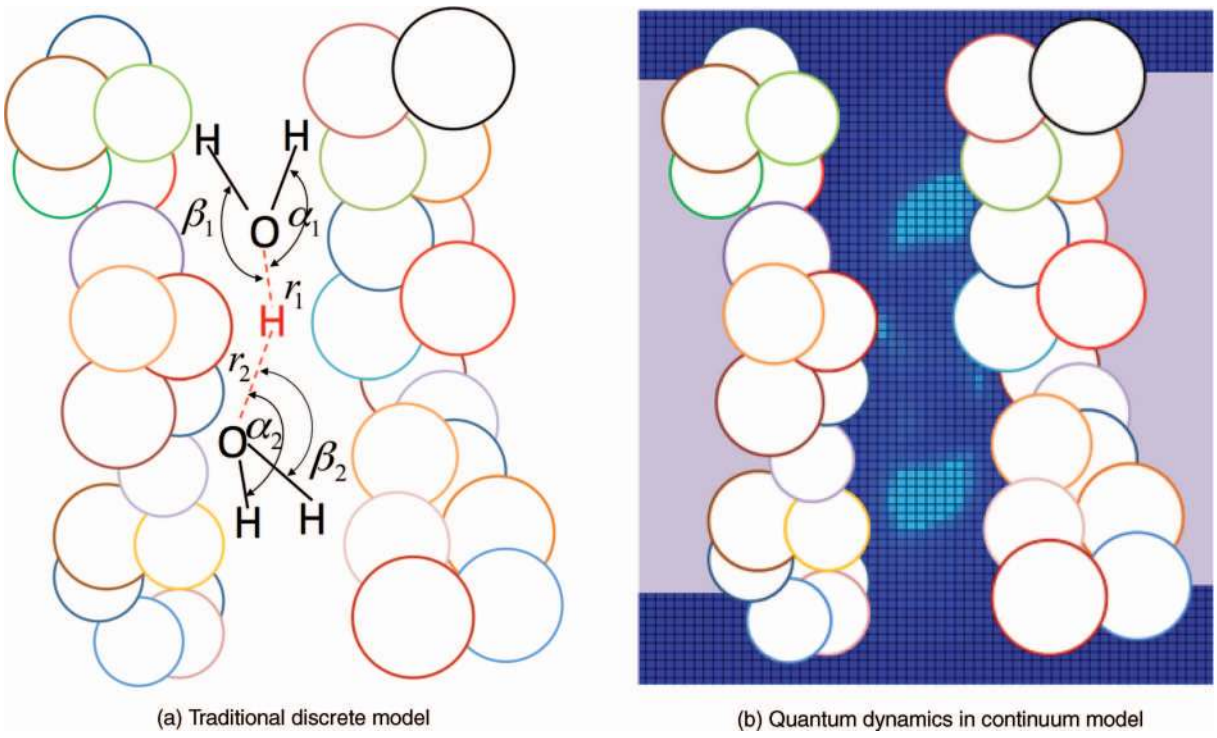

FIG. 2. Different strategies on treatment of proton-water interaction model.

models, from *ab initio*, quantum/semi-classical to molecular dynamics approaches. These treatments are obviously rich in details and are able to exhibit as much physical characteristics as possible. However, they are too computationally expensive to be employed for the entire proton transport process in realistic settings. Here we are seeking a balance between the simulation efficiency and biological details, by utilizing the spirit of multiscale quantum dynamics in continuum to incorporate the generalized correlation in reduced forms. All particles that may have non-electrostatic interactions with protons, including proton themselves, other ion species, water molecules, and fixed atoms of the channel protein, are all described in terms of number densities other than individuals in the generalized correlation. Nevertheless, the number density of protons is evaluated by a novel DFT via a new Kohn-Sham equation.

In our approach, the free energy functional of short-range interactions is modeled as a function of the local ion density $n(\mathbf{r})$ and the density gradient ∇n, i.e., $U_{\mathrm{GC}}[n, \nabla n]$

$$G_{\mathrm{GC}}[S, n] = \int (1 - S(\mathbf{r}))U_{\mathrm{GC}}[n, \nabla n]d\mathbf{r}. \tag{3}$$

We start from the assumption that the ∇n dependence has been omitted as a first order approximation, and then the $U_{\mathrm{GC}}[n]$ is classified into proton-proton, proton-other mobile ions, proton-water and proton-protein interactions, i.e.,

$$G_{\mathrm{GC}}[S, n] = \frac{1}{2}\int\int (1 - S(\mathbf{r}))n(\mathbf{r})n(\mathbf{r}')K_p(\mathbf{r} - \mathbf{r}')d\mathbf{r}'d\mathbf{r} \tag{4}$$

$$+ \sum_{j=1}^{N_c'}\int\int (1 - S(\mathbf{r}))n(\mathbf{r})n_j'(\mathbf{r}')K_j(\mathbf{r} - \mathbf{r}')d\mathbf{r}'d\mathbf{r} \tag{5}$$

$$+ \int\int (1 - S(\mathbf{r}))n(\mathbf{r})n_w(\mathbf{r}')K_w(\mathbf{r} - \mathbf{r}')d\mathbf{r}'d\mathbf{r} \tag{6}$$

$$+ \sum_{i=1}^{N_a}\int (1 - S(\mathbf{r}))n(\mathbf{r})n_i(\mathbf{r}')K_i(\mathbf{r} - \mathbf{r}')d\mathbf{r}, \tag{7}$$

where functions of proton number density $n(\mathbf{r})$ and all other ion species $n_j'(\mathbf{r})$ follow the previous definitions. We define the number density of each fixed atom of the channel protein as $n_i(\mathbf{r}) = \delta(\mathbf{r} - \mathbf{r_i})$ and the water density $n_w(\mathbf{r})$ will be discussed later. From Eqs. (4)–(7), it is easy to see that all short-range interactions are in a uniform structure, i.e., the integral of product between proton number density, the number density of the environments and the corresponding interaction kernels. By taking variation with respect to the proton number density, one obtains the generalize correlation potential, i.e.,

$$\begin{aligned}\frac{\partial U_{\mathrm{GC}}[n, \nabla n]}{\partial n} &= V_{\mathrm{GC}}(\mathbf{r}) \\ &= n(\mathbf{r}) * K_p(\mathbf{r}) + \sum_{j=1}^{N_c'} n_j'(\mathbf{r}) * K_j(\mathbf{r}) \\ &\quad + n_w(\mathbf{r}) * K_w(\mathbf{r}) + \sum_{i=1}^{N_a} n_i(\mathbf{r}) * K_i(\mathbf{r}),\end{aligned} \tag{8}$$

where * represents the convolution operation.

In the current work, we explore more sophisticated models for the V_{GC}. The kernel function $K_\alpha(\mathbf{r})(\alpha = \{i, j, p, w\}) : \mathbb{R}^3 \to \mathbb{R}$ is assumed to be continuous and have the following properties:

$$K_\alpha(\mathbf{r}) \in L^1(\mathbb{R}^3) \cap L^2(\mathbb{R}^3); \tag{9}$$

$$\lim_{|\mathbf{r}|\to\infty} K_\alpha(\mathbf{r}) \sim o(|\mathbf{r}|^{-2}); \tag{10}$$

$$\lim_{|\mathbf{r}|\to 0} K_\alpha(\mathbf{r}) \to \infty. \tag{11}$$

Property (9) ensures the boundedness of integrals of the kernel with other possible constant number densities and overall energy functional. Property (10) indicates the behavior of fast decay or short-range interactions, while the last one prevents the overlapping of particle centers. The Pauli repulsion term should grow much faster than any attractive term as $|\mathbf{r}| \to 0$. An easy and direct construction of the interaction kernel would be

$$K_\alpha(\mathbf{r}) = \sum_{k=3}^{\infty} c_k^\alpha |\mathbf{r}|^{-k} \tag{12}$$

with c_k^α being fitting parameters necessary to various experimental observations. In fact, this formulation covers the Lennard-Jones potential and its variants for interactions between various particles. Some specific forms of this general expression are also adopted in modeling the discrete proton-water interactions.[50]

In the present work, in order to reduce the size of the parameters set, we conveniently consider the 12-6 Lennard-Jones pair potential kernel of form

$$K_\alpha(\mathbf{r}) = \bar{\epsilon}_\alpha\left[\left(\frac{\sigma_p + \sigma_\alpha}{|\mathbf{r}|}\right)^{12} - 2\left(\frac{\sigma_p + \sigma_\alpha}{|\mathbf{r}|}\right)^{6}\right] \tag{13}$$

where $\bar{\epsilon}_\alpha$ is the well-depth parameter and σ_α is the radius parameter of ions or atoms. With this simplification, one can spell out the components of the $V_{\mathrm{GC}}(\mathbf{r})$,

$$\begin{aligned}V_{\mathrm{GC}}(\mathbf{r}) = \bar{\epsilon}_p\int n(\mathbf{r}')\left[\left(\frac{2\sigma_p}{|\mathbf{r} - \mathbf{r}'|}\right)^{12} - 2\left(\frac{2\sigma_p}{|\mathbf{r} - \mathbf{r}'|}\right)^{6}\right]d\mathbf{r}' \\ + \sum_{j=1}^{N_c'}\bar{\epsilon}_j\int n_j'(\mathbf{r}')\left[\left(\frac{\sigma_p + \sigma_j}{|\mathbf{r} - \mathbf{r}'|}\right)^{12} - 2\left(\frac{\sigma_p + \sigma_j}{|\mathbf{r} - \mathbf{r}'|}\right)^{6}\right]d\mathbf{r}' \\ + \bar{\epsilon}_w\int n_w(\mathbf{r}')\left[\left(\frac{\sigma_p + \sigma_w}{|\mathbf{r} - \mathbf{r}'|}\right)^{12} - 2\left(\frac{\sigma_p + \sigma_w}{|\mathbf{r} - \mathbf{r}'|}\right)^{6}\right]d\mathbf{r}' \\ + \sum_{i=1}^{N_\alpha}\bar{\epsilon}_i\left[\left(\frac{\sigma_p + \sigma_i}{|\mathbf{r} - \mathbf{r}_i|}\right)^{12} - 2\left(\frac{\sigma_p + \sigma_i}{|\mathbf{r} - \mathbf{r}_i|}\right)^{6}\right].\end{aligned} \tag{14}$$

Although the Lennard-Jones formulation is utilized as the interaction kernels, the GC in our work is significantly different from the conventional Lennard-Jones potential. First

of all, Lennard-Jones potential is traditionally formulated to model short-range interactions between two individual particles. While the current GC is more general, it could represent particle-particle interactions. More importantly, it includes continuum-continuum (proton-ion and proton-water) interactions and continuum-discrete (proton-protein) interactions.[58] Another aspect is that the description of the proton number density is quantum mechanical. There is much literature for the study of proton interactions in full atomic details with either quantum mechanics or classical mechanics. However, to our knowledge, it is the first time that quantum dynamics is built into the multiscale (discrete and continuum) formulation of the complex heterogeneous system in order to balance accuracy and efficiency. In other words, the formulation of the GC is also proposed in the spirit of our quantum dynamics in continuum. The finite size effect of ions in the narrow channel is naturally described in the GC formulation. More importantly, ion-water interactions are quantitatively formulated in our ion channel model. The ion-water interaction is critical to the channel selectivity among ions with the same charge and the essential translocation mechanism of protons. For regular ions, they exist in the solvent as ion-water clusters. When ions diffuse from bulk water to a relatively narrow channel, they have to undergo the dehydration process. Such a process poses an additional energy barrier, because the presence and/or motion of water molecules in a narrow channel are greatly restricted, and some physical characteristics, such as oxygen-oxygen distance, water orientation angle, will be significantly different from those in the bulk region. For protons, forming and breaking hydrogen bonds in a narrow channel will be different for those in the bulk water. The proceeding paragraphs are contributed to demonstrate how this GC formulation can reveal the difference of proton-water interactions in the bulk solvent and the narrow channel pore.

III. GOVERNING EQUATIONS AND THEIR SOLUTION

In this section, the governing equations for S, Φ, and Ψ_E are derived from the total free energy functional with the GC component by the variational principle via the Euler-Lagrange equation.[23] Computational algorithms and procedures for the solution of governing equations are also discussed.

A. Generalized Laplace-Beltrami (LB) equation

By variation of Eq. (1) with respect to the characteristic function $S(\mathbf{r})$, we have

$$\frac{\delta G_{\text{total}}[S,\Phi,n]}{\delta S} = 0 \Longrightarrow -\nabla\cdot\left(\gamma\frac{\nabla S}{|\nabla S|}\right) - V_{\text{LB}} = 0, \tag{15}$$

where $\nabla\cdot\left(\gamma\frac{\nabla S}{|\nabla S|}\right)$ is a generalized Laplace-Beltrami operator, which is a generalization of the usual Laplacian operator to a smooth manifold of the solvent-macromolecular interface[23,59] and the generalized Laplace-Beltrami (LB) potential V_{LB} is defined as

$$\begin{aligned} V_{\text{LB}} = &-p + \rho_0 U_{ss} + \left[\frac{\epsilon_m}{2}|\nabla\Phi|^2 - \Phi\rho_f\right] \\ &- \left[\frac{\epsilon_s(\mathbf{r})}{2}|\nabla\Phi|^2 - \Phi n(\mathbf{r})q + k_B T\sum_j^{N_c'} n_j^0\left(e^{-\frac{q_j\Phi-\mu_j}{k_B T}} - 1\right)\right] \\ &+ \left[\int\frac{\hbar^2 e^{-(E-\mu_p)/k_B T}}{2m(\mathbf{r})}|\nabla\Psi_E(\mathbf{r})|^2 dE + U_{\text{GC}}[n] + U_{\text{Ext}}[n]\right] \\ &- \lambda\left[\int e^{-\frac{E-\mu_p}{k_B T}}|\Psi_E(\mathbf{r})|^2(\mathbf{r})dE - \frac{N_p}{V_\Omega}\right]. \end{aligned}$$

Generally, Eq. (15) can be solved by introducing an artificial time to obtain an alternative parabolic partial differential equation of $\bar{S}:\Omega\times[0,\infty)\mapsto\mathbb{R}$:

$$\frac{\partial\bar{S}}{\partial t} = |\nabla\bar{S}|\left[\nabla\cdot\left(\gamma\frac{\nabla\bar{S}}{|\nabla\bar{S}|}\right) + V_{\text{LB}}\right], \tag{16}$$

with boundary condition

$$\bar{S}(\mathbf{r}) = 0, \forall\mathbf{r}\in\partial\Omega\times[0,\infty)$$

and initial condition

$$\bar{S}(\mathbf{r},0) = \begin{cases} 1, & \mathbf{r}\in D_{\text{m}} = \bigcup_{i=1}^{N_a}\{\mathbf{r}:|\mathbf{r}-\mathbf{r}_i| < r_i^{\text{VDW}} + r_p\} \\ 0, & \text{otherwise,}\end{cases} \tag{17}$$

where r_i^{VDW} and r_p are atomic van der Waals radius and the probe radius, respectively. The solution to Eq. (15) is given by $S(\mathbf{r}) = \bar{S}(\mathbf{r})$ at the steady state: $\partial\bar{S}/\partial t = 0$. We have developed this approach for the construction of biomolecular surfaces over many years;[58–61] also see Ref. 62 for similar work.

B. Generalized Poisson-Boltzmann (PB) equation

The governing equation for the electrostatic potential can be derived by the variation of energy functional (1) with respect to electrostatic potential Φ

$$\frac{\delta G_{\text{Total}}[S,\Phi,n]}{\delta\Phi} = 0 \Longrightarrow -\nabla\cdot(\epsilon(S)\nabla\Phi(\mathbf{r})) - (1-S)\sum_{j=1}^{N_c'} n_j^0 e^{-\frac{q_j\Phi(\mathbf{r})-\mu_j}{k_BT}} = (1-S)n(\mathbf{r})q + S\rho_f(\mathbf{r}). \tag{18}$$

Equation (18) is a generalized Poisson-Boltzmann equation[23,58] describing the electrostatic potential with three types of charge sources: the ions of interest, other ions species in the solvent described by the continuum approximation (i.e., Boltzmann distribution) and fixed point charges in biomolecules. This equation is not closed because $S(\mathbf{r})$ and $n(\mathbf{r})$ need to be evaluated from other governing equations. Equation (18) is presented in the so-called Eulerian formulation, which offers a smooth surface profile of the biomolecule.[23,58] A Lagrangian formulation[54] of our variational approach has also been derived, which gives rise to a sharp interface Γ. In practice, one can obtain a Lagrangian representation of the VSI from the Eulerian formulation by setting a level set of the characteristic function S, namely, $\Gamma = \{\mathbf{r}\in\mathbb{R}^3 | S(\mathbf{r}) = c\}$, where $0 < c < 1$ is a constant. With this algorithm, the electrostatic potential $\Phi(\mathbf{r})$ solves the following generalized PB equation at the VSI limit:

$$-\nabla\cdot(\epsilon(\mathbf{r})\nabla\Phi(\mathbf{r})) - \sum_{j=1}^{N_c'} q_j n_j^0 e^{-\frac{q_j\Phi-\mu_j}{k_BT}} = qn(\mathbf{r}) + \sum_{i=1}^{N_a} Q_i\delta(\mathbf{r}-\mathbf{r}_i), \tag{19}$$

subject to the following jump conditions,

$$[\Phi]|_\Gamma = \Phi^+(\mathbf{r}) - \Phi^-(\mathbf{r}) = 0, \tag{20}$$

$$[\epsilon\nabla\Phi\cdot\vec{\mathbf{n}}]|_\Gamma = \epsilon^+\nabla\Phi^+(\mathbf{r})\cdot\vec{\mathbf{n}} - \epsilon^-\nabla\Phi^-(\mathbf{r})\cdot\vec{\mathbf{n}} = 0, \tag{21}$$

and mixed boundary conditions

$$\Phi(\mathbf{r}) = V_{\text{Ext}}, \forall\mathbf{r} \text{ on predefined electrode region of } \partial\Omega$$
$$\frac{\partial\Phi(\mathbf{r})}{\partial\vec{\mathbf{n}}} = 0, \forall\mathbf{r} \text{ on other part of } \partial\Omega,$$

where V_{Ext} is the external electric voltages on the electrodes, superscripts "+" and "−" represent the limiting values of a certain function at two sides of interface Γ, and $\vec{\mathbf{n}}$ is the unitary outward normal direction of Γ or $\partial\Omega$.

Consequently, Eqs. (20) and (21) guarantee the continuities of the potential function and its flux. Equation (19) has discontinuous coefficient $\epsilon(\mathbf{r})$ across the sharp interface Γ, which is very complex in general for biomolecules. Additionally, charge sources consist of a large number of delta functions, which may cause computational difficulties. Fortunately, all of the above-mentioned challenges can be successfully handled by our MIB method[43–46] and our DNM scheme.[16,45]

C. Generalized Kohn-Sham (KS) equation

In the present multiphysics model, the proton number density $n(\mathbf{r})$ in Eq. (18) is related to the wavefunction $\Psi_E(\mathbf{r})$, which is governed by the generalized Kohn-Sham equation. This equation is obtained by the variation of the total free energy functional (1) with respect to wavefunction $\Psi_E^\dagger$

$$\frac{\delta G_{\text{Total}}[S,\Phi,n]}{\delta\Psi_E^*} = 0 \Longrightarrow -\nabla\cdot\frac{\hbar^2}{2m(\mathbf{r})}\nabla\Psi_E(\mathbf{r}) + V(\mathbf{r})\Psi_E(\mathbf{r}) = E\Psi_E(\mathbf{r}), \tag{22}$$

where we set the Lagrange multiplier $\lambda = E$. The total Hamiltonian of the proton is given by

$$H = -\nabla\cdot\frac{\hbar^2}{2m(\mathbf{r})}\nabla + V(\mathbf{r}), \tag{23}$$

in which the total effective potential energy

$$V(\mathbf{r}) = q\Phi(\mathbf{r}) + V_{\text{GC}}(\mathbf{r}) + V_{\text{Ext}}(\mathbf{r}) \tag{24}$$

consists of electrostatic, generalized correlation and external contributions. The external potential can be omitted for a closed system without external fields.

It is important to note that generalized Kohn-Sham equation (22) is fundamentally different from the normal Kohn-Sham equation for electronic structures. The Kohn-Sham operator in Eq. (22) has an absolutely continuous spectrum and invokes the Boltzmann statistics for proton scattering. Whereas the normal Kohn-Sham operator has a discrete spectrum and assumes the Fermi Dirac statistics for electron occupations (bound states).

One of important quantum observables, the proton current, is defined by standard probability flux, whose practical expression is the following

$$I = \frac{q}{h}\text{Tr}\int G(E)V_{\text{intra}}^{ah}G^\dagger(E)V_{\text{extra}}^{ah}[e^{-\frac{E-\mu_{\text{extra}}}{k_BT}} - e^{-\frac{E-\mu_{\text{intra}}}{k_BT}}]dE. \tag{25}$$

where Tr is the trace operation, G is the Green's operator

$$G(E) = (E-H)^{-1}, \tag{26}$$

and μ_{extra} and μ_{intra} are the external electrical field energies at extracellular and intracellular electrodes, respectively. Here V_{extra}^{ah} and V_{intra}^{ah} are the anti-Hermitian components of the external potentials.[16]

It is worthwhile to emphasis that Eqs. (15), (18), and (22) are closely coupled. Both the generalized PB and KS equations depend on the VSI, which is generated from the characteristics function $S(\mathbf{r})$. Furthermore, the proton number density $n(\mathbf{r})$, which is the solution of the generalized KS equation, serves as part of the charge source in the PB equation, while the electrostatics $\Phi(\mathbf{r})$ is part of the Hamiltonian of the proton. Finally, both the proton number density and electrostatics appear in the generalized LB equation to determine the characteristics function. This coupled system endows us the

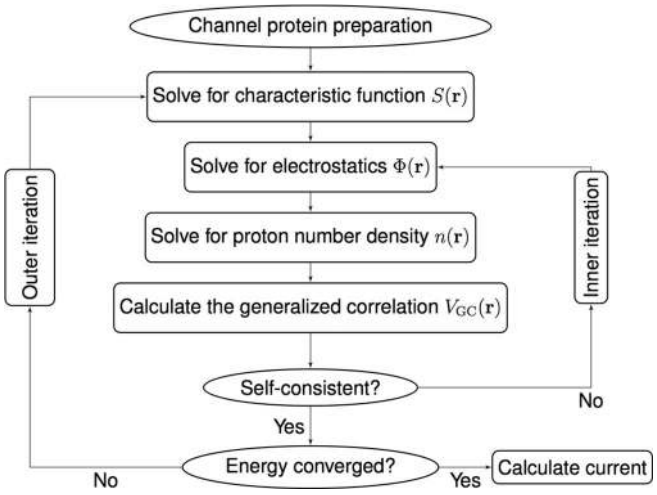

FIG. 3. Work flow of the overall surface driven self-consistent iteration.

flexibility to deal with complex multiphysics in a multiscale fashion — the quantum dynamics in continuum model.

D. Solution protocol

Equations (15), (18), and (22) form a strongly coupled system and they need to be solved iteratively. This situation results in a nonlinear system with three variables. One needs to predetermine two of them to solve for the third one and the whole loop is a complex self-consistent iteration procedure. In our earlier work,[17] a surface driven dynamical iteration procedure is proposed to solve the system of three governing equations. In this tactic, the characteristic function $S(\mathbf{r})$ serves as the leading variable in the dynamic evolution that initiates the internal self-consistent iteration of $\Phi(\mathbf{r})$ and $n(\mathbf{r})$.[16,54,55,58] The overall iteration is outlined as the following:

- **Step 0.** Preparation. All the necessary preparations for the whole loop are accomplished in this step, which include:
  - 0.1. The channel protein of interest is downloaded from the Protein Data Bank (PDB). Partial charges, positions, radii of all atoms are determined by a certain force field such as CHARMM (Ref. 26) and related software packages, such as PDB2PQR.[63] The prepared channel structure is then embedded in a proper computational domain.
  - 0.2. Generate the initial condition $S(\mathbf{r}, 0)$ according to Eq. (17) for Eq. (16).
- **Step 1 (Surface dynamics).** Solving the generalized Laplace-Beltrami equation with $\Phi^m(\mathbf{r})$ and $n^m(\mathbf{r})$ (initial guess as zero if $m = 0$). Calculate total energy G^m_{Total}. Note that index m is for the external or surface driven dynamic evolution loop.
- **Step 2 (Self-consistent iteration).** This step is considered as the internal self-consistent iteration of electrostatics $\Phi^{m,l}(\mathbf{r})$ and proton number density $n^{m,l}(\mathbf{r})$, where superscripts l is added for the internal iteration:
  - 2.1. Solve generalized Poisson-Boltzmann equation to attain updated $\Phi^{m,l+1}(\mathbf{r})$.
  - 2.2. Calculate the generalized correlation using $n^{m,l}(\mathbf{r})$ with designed correlation kernels.
  - 2.3. Solve generalized Kohn-Sham equation to attain new density $n^{m,l+1}(\mathbf{r})$.
- **Step 3 (Self-consistent convergence check).** If $||\Phi^{m,l+1} - \Phi^{m,l}|| < \varepsilon_1$ and $||n^{m,l+1} - n^{m,l+1}|| < \varepsilon_2$, where ε_1 and ε_2 are predefined internal error tolerances, set $\Phi^{m+1}(\mathbf{r}) = \Phi^{m,l+1}$, $n^{m+1}(\mathbf{r}) = n^{m,l+1}(\mathbf{r})$ and go to Step 4, otherwise go to Step 2.1.
- **Step 4 (Dynamic energy convergence check).** Update energy G^{m+1}_{Total} with $S^{m+1}(\mathbf{r})$, $\Phi^{m+1}(\mathbf{r})$. If the total energy is convergent, go to Step 5 otherwise go to Step 1.
- **Step 5 (Proton current calculation).** Calculate the proton current by Eq. (25).

Figure 3 gives an explicit graphic illustration of the above work flow.

IV. RESULTS AND DISCUSSIONS

In this section, we carry out numerical experiments of the proposed multiscale/multiphysics QDC model with the GC. We first explore the behavior of the GC potentials. As discussed in Sec. II B, the present GC involves the evaluation of the Lennard-Jones potential over the continuum domain, which differs very much from the usual two-particle definition of the Lennard-Jones potential.

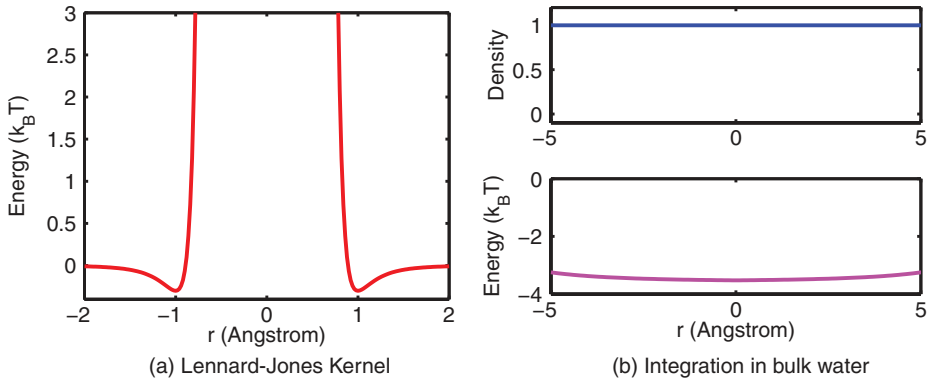

(a) Lennard-Jones Kernel (b) Integration in bulk water

FIG. 4. A typical Lennard-Jones kernel and its interaction property in the bulk water.

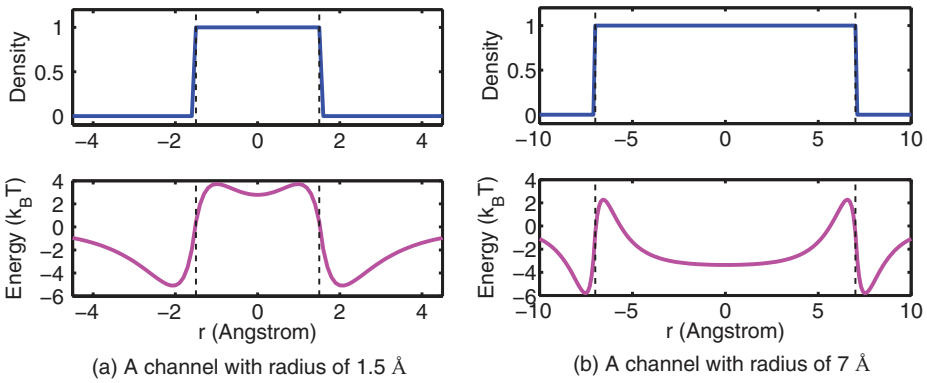

FIG. 5. A 1D demonstration of geometric confinement effects on ion-water interaction potential energy. Channel width is represented between the two vertical dashed lines. (a) A narrow channel; (b) A wide channel.

The validity of the proposed model for proton transport and related performance analysis are presented based on a specific channel protein, the Gramicidin A (GA, PDB code: 1MAG). For simulation simplify, the solvent is considered as hydrogen chloride (HCl), i.e., only protons and Cl^- are mobile ions. Unless specified, the parameters of the governing equations in current work admit the same values as those in our earlier work.[17]

A. Generalized correlations

In this subsection, we investigate the properties of the GC by considering geometric effects, size effects, the effect of solvent distribution, etc. For the purpose of illustration, we consider two cases, a uniform distribution and a Gaussian distribution of the water density in the channel pore. Comparison is given to the GC in the bulk water.

Figure 4 gives an illustration of a typical 12-6 Lennard-Jones kernel and its convolution with a constant function, which represents the water density (normalized as one) in the bulk water region. Figure 4(a) depicts the profile of the Lennard-Jones potential. The upper panel of Fig. 4(b) gives the number density of water molecules and the lower panel shows the proton-water interaction of the GC as convolution of the number density and the interaction kernel. When the water density is a constant in bulk region, one can essentially obtain the interaction energy of water molecules and ions as a predefined constant in the bulk, by choosing appropriate parameters.

Figure 5 shows the GC of proton and water molecules in a channel pore in a 1D demonstration. The upper panels of Fig. 5 indicate the water densities in a narrow channel and a wide one. The water density is simply taken as one in channel region while zero in protein region. By the convolution of the functions in the upper panel of Fig. 5 with the kernel in Fig. 4(a), one can obtain the interaction potential functions in the lower panels. It can be easily found out that for an extremely narrow channel with a radius of 1.5 Å, the proton-water interaction yields a moderately large energy barrier. While for a wider channel with a radius of 7.0 Å, the energy barrier is relatively low, similar to that in the bulk region, except near the channel wall. This comparison explains the geometric confinement or size effect of the channel pore. When the channel pore is relatively wide, as shown in Fig. 5(b), the geometric confinement is not intense and the proton-water interaction tends to be similar to that in the bulk solvent. However, when strong geometric confinement occurs, which usually results from a narrow channel pore, the interaction function changes and serves as a large energy barrier.

Figure 6 shows a similar profile for a channel of radius 2.0 Å, which is the typical size of a proton channel pore, but with two different assumptions of the water density. In

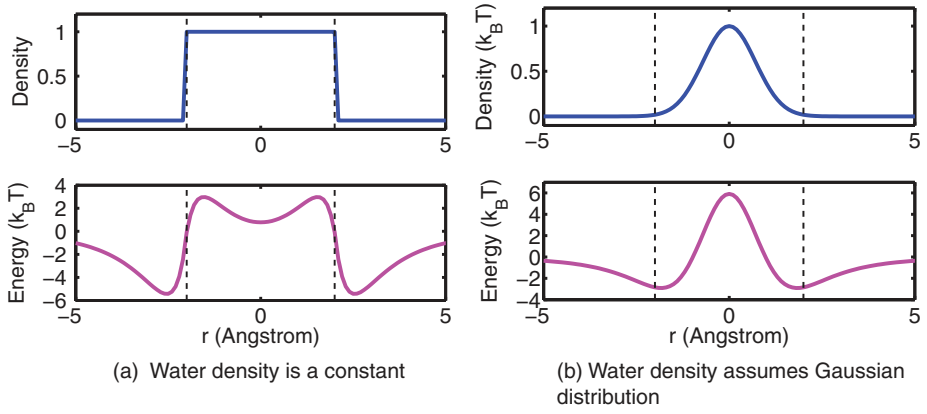

FIG. 6. A 1D demonstration of geometric confinement effects on ion-water interaction with different water density distribution. Channel width is represented between the two vertical dashed lines. (a) Constant water density and energy profile; (b) Water density in Gaussian distribution and energy profile.

Fig. 6(a), the water density is still assumed as a constant in the channel (upper panel), and the energy profile is similar to that of Fig. 5(a), but with a lower barrier in the middle. We next consider the Gaussian distribution, which is a more suitable assumption of water density in the narrow channel.[64] As indicated in the Fig. 6(b), an energy barrier is also formed in the channel region while it is more concentrated in the middle, as expected.

B. Proton transport in Gramicidin A

The GA channel protein exists in the soil bacterial species *Bacillus brevis* and is one of the best studied ion channels, both structurally and functionally. The GA is a dimer in a bilayer membrane, and consists of two head-to-head β-helical parts. Two parts of the dimer have an identical sequence: FOR-VAL-GLY-ALA-DLE-ALA-DVA-VAL-DVA-TRP-DLE-TRP-DLE-TRP-DLE-TRP-ETA. It forms a narrow pore of about 4 Å in diameter and 25 Å in length. The GA is known to select small monovalent cations, and bind bivalent cations, while rejecting anions. Due to its well-defined structure and abundant experimental data, the GA has been used as a testbed for highly accurate numerical algorithms[13] and newly developed Poisson-Boltzmann-Nernst-Planck model in our earlier work.[18] Indicated by sufficiently many experimental evidences, the GA is a water-filled pore in which roughly twelve water molecules are aligned. Hydrogen-bonded chain can form within the single file of water molecules, which sustains proton transport through the Grotthuss-type mechanism. Because of the simple structure and fruitful biological conclusion of the GA, we utilize it to validate the proposed model and algorithms.

1. Electrostatic properties

First, we examine the surface electrostatic distribution in the GA channel protein. Figure 7 shows the calculated electrostatic potential mapped on the VSI in this system. Although the GA is neutral in general, its surface electrostatic potential is mostly negative near the channel mouth as indicated by the red color in the graph. Furthermore, as shown in Fig. 7(b), the inner wall of the channel pore is also intensively negatively charged. This fact indicates the obvious selectivity of the GA channel — it selects cations and suppresses anions.

The electrostatics of the channel system greatly depends on the dielectric constants used in Eq. (18). We have explored a proper range of the dielectric constant of each component in biological sense and tested a wide range of values in order to obtain a reasonable prediction in our earlier work.[16] The study on the dielectric constant ϵ_m of the molecule in the ion transport problem is quite fruitful and there is a general agreement that ϵ_m could be taken as a constant that slightly greater than 2, which is the value used in the solvation study. While the dielectric constant ϵ_s for the solvent should be position dependent. The dielectric constant $\epsilon_{\text{bath}} = 80$ is the value widely accepted in the literature for the bath water region. However, since the mobility of the water molecules in the channel pore is restricted because of the small radius, the dielectric constant ϵ_{ch} remains mysterious and various values are tested in reported simulations.[16]

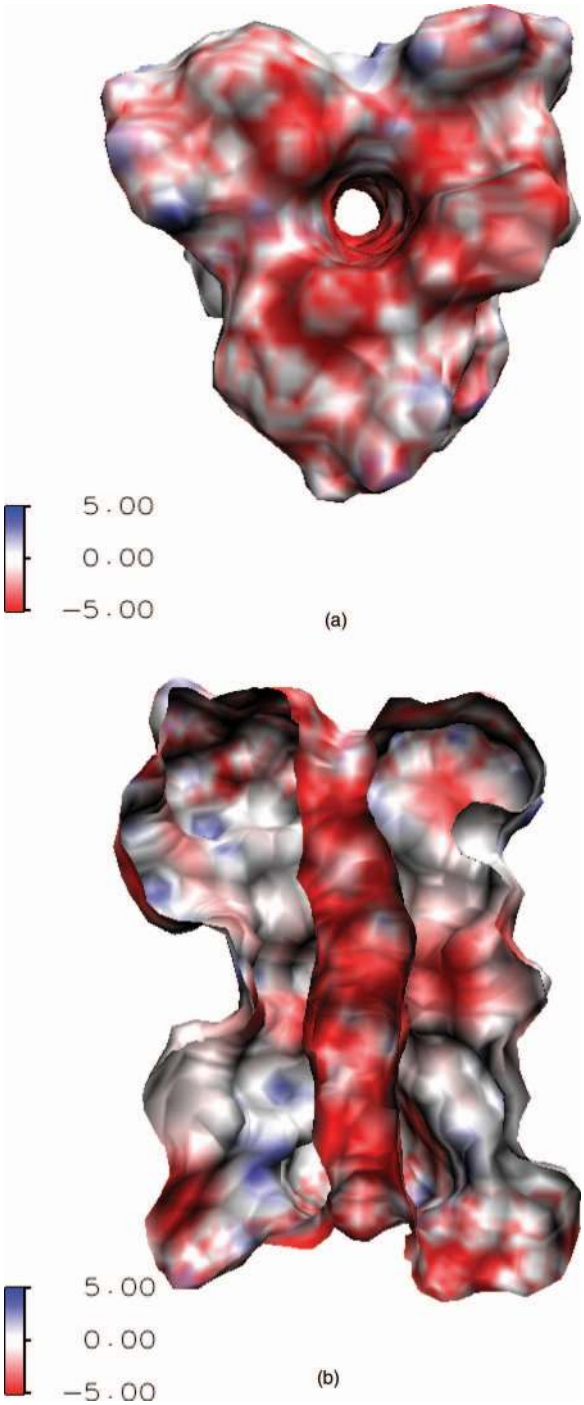

FIG. 7. 3D illustration of the Gramicidin A (GA) channel structure and surface electrostatic potential. The negative surface electrostatics as indicated by the intensive red color on the channel upper surface and inside the channel pore implies that the GA selects positive ions. (a) Top view of the GA channel; (b) Side view of the GA channel.

Figure 8 quantitatively displays the electrostatic potential of the GA channel with three different values of ϵ_{ch}. All quantities are averaged on the cross section along the channel axis, although the original data is calculated in 3D. Here ϵ_m is taken as 5 and the reference ionic density is set to 0.1 M. The vertical dashed lines indicate the entrance (left) and exit (right) of

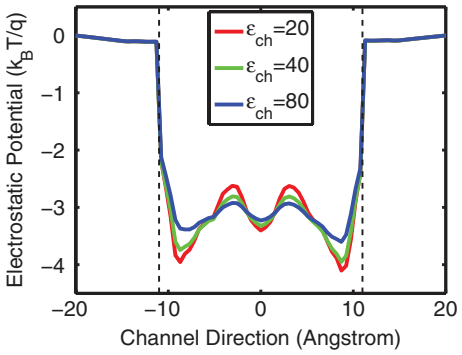

FIG. 8. Electrostatic potential of the GA channel along the z-axis obtained with $\epsilon_m = 5$ and $n_p^0 = 0.1$ M (Red: $\epsilon_{\text{ch}} = 20$; Green: $\epsilon_{\text{ch}} = 40$; Blue: $\epsilon_{\text{ch}} = 80$).

the GA channel. Although the GA protein is overall neutral in charge, it possesses a negative environment in the channel region and this fact leads to a large potential well. Near the entrance and the exit of the channel, there are two local potential minima (the valley near the dashed line) and a major barrier in the middle of the channel. The magnitude of the electrostatic potentials responds directly to the change of ϵ_{ch} value. When ϵ_{ch} decreases from 80, which is the commonly used value for the solvent, to the smaller values suggested by biological observations, the contrast between the energy wells near the entrance/exit and the barrier in the middle becomes sharper. This phenomenon verifies the impact of ϵ_{ch} value and leads us to prefer a smaller value in our model.

2. Generalized correlation properties

Next, we check the calculated generalized correlation in a realistic situation. The parameters in Eq. (14) are the following: $\sigma_p = 0.644$ Å, $\sigma_w = 1.505$ Å, $\sigma_j = 1.81$ Å, and σ_i for each fixed atom is taken from the PDB data file. For those energy well depths, $\bar{\epsilon}_p = 0.0598$ kcal/mol, $\bar{\epsilon}_j = 0.0295$ kcal/mol, $\bar{\epsilon}_w = 0.0472$ kcal/mol, and $\bar{\epsilon}_i = 0.0173$ kcal/mol. Figure 9 shows the calculated generalized correlation mapped on the VSI. As one can see from Eq. (14), the value of GC depends on the corresponding number densities of particles and the parameter set. Since the GC mainly represents the interactions of particles, the finite size effect, the geometry confinement induced dehydration and restriction of water motion, it generally gives rise to a repulsive force or serves as an energy barrier to permeating ions (regardless of the sign of charge) near the surface, relative to the bulk property. This fact has been revealed in Fig. 9. Comparing to the intensive red color which indicates negative values of electrostatic potential energy in Fig. 7, the GC mapped on the channel surface is blue and positive. Figure 9(a) shows the GC in top view, from which one can conclude that when ions approach the mouth of the channel, they will response to the repulsive force from the GC. Figure 9(b) shows the situation in the channel, which also has intensively positive value of the GC, the energy barrier in the channel pore represents the geometric confinement.

Figure 10 gives detailed decomposition of the GC values averaged along the transport direction. The pink curve represents the interaction between proton and all mobile ions, including protons themselves and other ions. Since ionic density is low in the channel, the GC interaction strength is small in the channel comparing in the bulk solvent. The blue curve indicates the GC interaction between proton and water molecules. In the bulk region, the motion of water molecule is not confined and relatively free, therefore the interaction is small due to the homogeneous integration. However, because of geometric restriction of water density and degree of

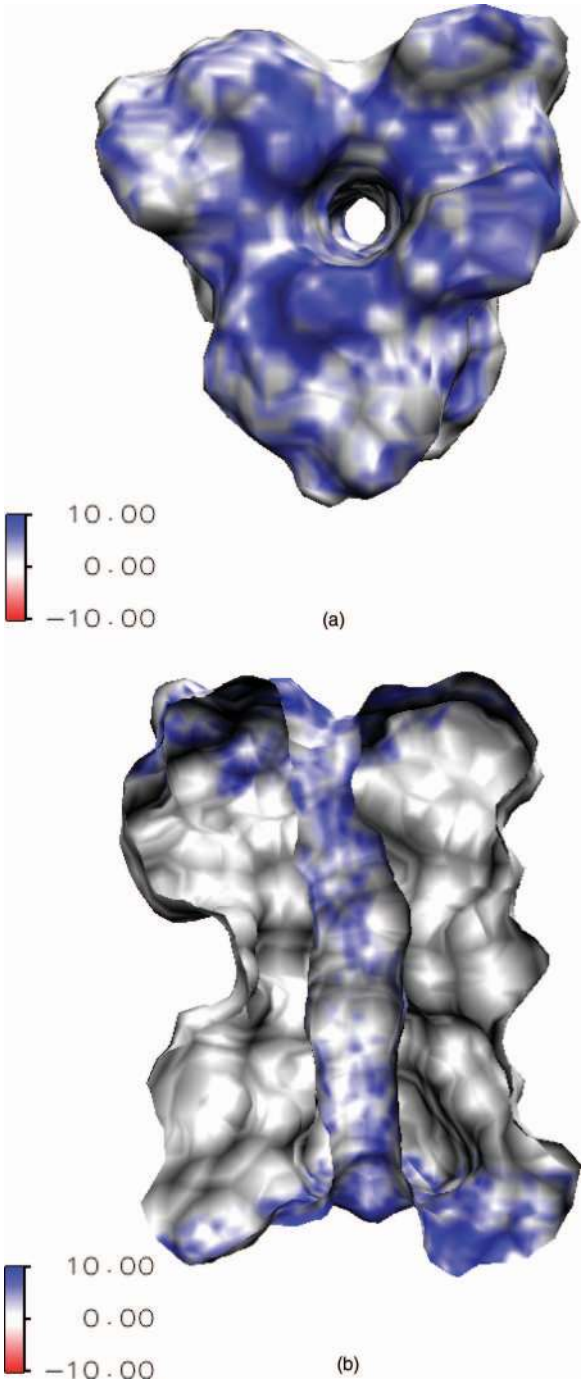

FIG. 9. Calculated generalized correlation mapped on the 3D GA channel surface. The positive surface generalized correlation as indicated by the intensive blue color on the channel upper surface and inside the channel pore implies that the GC usually generates a repulsive force. (a) Top view of the GA channel; (b) Side view of the GA channel.

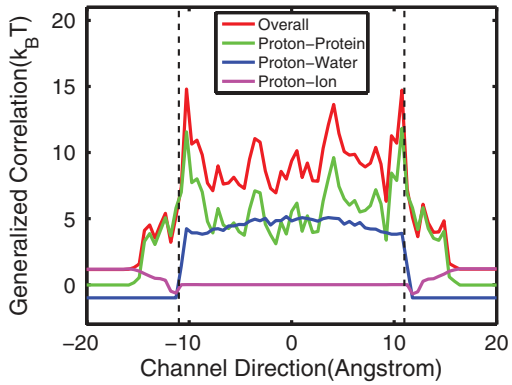

FIG. 10. Generalized correlation potentials of the GA channel along the z-axis.

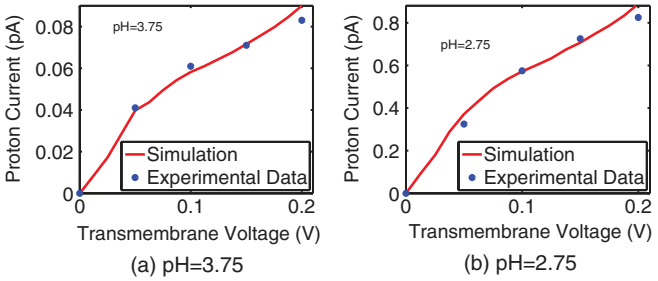

FIG. 12. Voltage-current relation of proton translocation of GA at different concentrations. Blue dots: experimental data of Eisenman *et al.* (Ref. 3); Red solid curves: QDC model prediction.

freedom of motion, this interaction is positive in the channel region. The green curve is the GC interaction between the proton and fixed channel protein atoms. It is easy to understand that this interaction is almost zero far away from the protein while may take big values in the narrow channel. Finally, the three types of GC potentials are summed up to the overall value, indicated by the red curve.

3. Proton conductivity

Before simulations and experimental data are compared, we check the total potential energy of the GA channel that an ion experiences during transport. The overall potential energy, i.e., sum of the electrostatics and the GC can quantitatively explain the transport mechanism and some aspect of channel selectivity. Figure 11 shows the total effective potential with contributions from both the electrostatics and generalized correlation under different voltage biases. Figure 11(a) is for the monovalent cations while Fig. 11(b) is for monovalent anions. It is agreed that the channel protein structure, or total potential field determines whether a specific ion can permeate the channel or not. Based on previous discussion and this figure one can conclude that the GC always results in an energy barrier in the channel pore, and its magnitude depends on the geometric confinement of the channel wall. On the other side, electrostatics facilitates the ionic permeation if the sign is right. Since the GA channel wall presents negative electrostatics, it is an energy well for the monovalent cations. Therefore, the combination of negative electrostatic energy with the positive GC forms a potential energy that allows cations to permeate. In contrast, the negative electrostatics yields an energy barrier for anions, the accumulation with the energy barrier of the GC forms a huge barrier that prevent any anions entering the channel.

Figure 12 displays simulated results of proton conductance through Eq. (25), compared with experimental data from the literature[14] of the GA channel. The blue dots in each figure represent available experimental observations for certain voltage biases, while the red curves are our QDC model predictions calculated with sufficiently many voltage samples. The model parameters are chosen to match the experimental data but all of the choices are taken within the range of physical measurements. Taking into account above considerations, we can conclude that the present predictions agree with experimental data quite well. This quantitative agreement validates our GC formulation and quantum dynamics in continuum model.

Apart from I-V curves, conductance-concentration relation (C-C curve) is another measurement under given voltages for proton transport. Figure 13 illustrates such a relationship with a comparison between experimental data and model predictions. The conductance of the channel is calculated with various proton concentrations as indicated by the horizontal

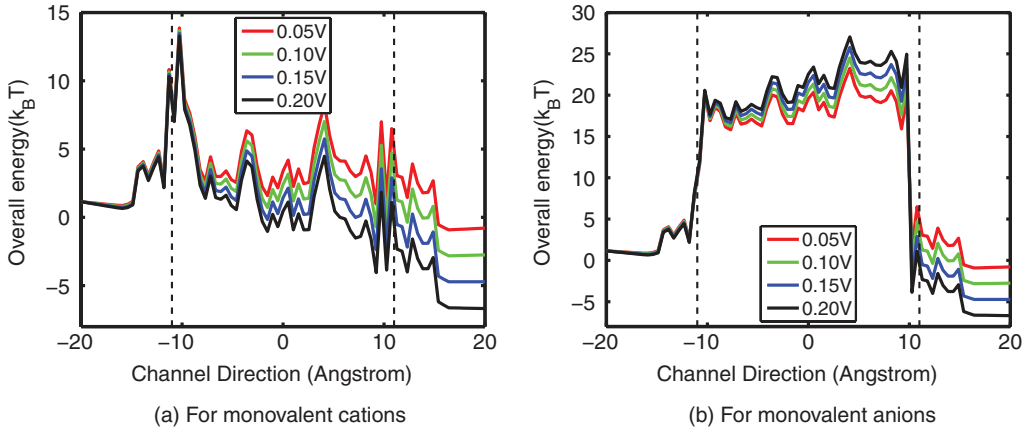

FIG. 11. Total potential energy of the GA channel, including electrostatic and generalized correlation contributions under various voltage biases. The *p*H value of solution is 2.75. (a) Total potential of monovalent cations; (b) Total potential of monovalent anions.

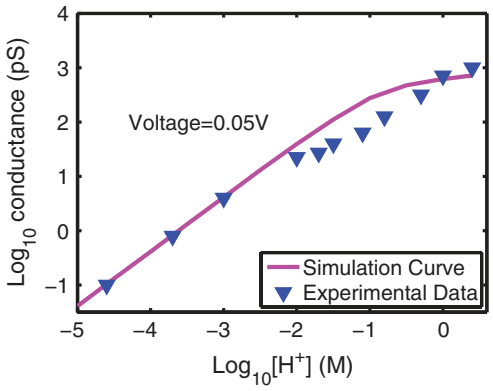

FIG. 13. Conductance-concentration relation of proton translocation at a fixed voltage. Voltage bias = 0.05 V; Blue triangles: experimental data of Eisenman *et al.* (Ref. 3); Red curve: QDC model prediction.

axis at a given voltage bias. The conductance-concentration relation is computed with the same set of parameters as that in Fig. 12. At lower proton concentrations (i.e., *p*H value greater than 2), the agreement between our prediction and experimental data is quite good. At relatively higher concentrations, the conductance saturates against the concentration as expected. It corresponds to the sub-linear characteristics or the flat tail of the C-C curve. The numerical simulations slightly overestimate the observed conductance between *p*H values of 1 and 2. Actually, the "shoulder" region exhibited in experimental data between *p*H values 1 and 2 (or the −2 and −1 of the $\log_{10}[H^+]$) is considered as changes in the rate-determining mechanism from the Grotthuss-type one to the hydrodynamic conduction of hydronium ions.[36] This aspect is not reflected in our current model and needs to be investigated in the future.

V. CONCLUDING REMARKS

Proton transport across lipid membrane plays a significant role in living cells. However, it is an extremely complicated system. When the membrane protein presents, this system contains solvation process, transport dynamics, quantum effects and protein structures, which all obey fundamental laws of nature. The diversity of physical principles and different level of interest in each component of the system require multiscale and multiphysics treatments in modeling and simulation. An innovative model, the QDC model, which includes a basic formulation with the VSI,[16,17] has been proposed to study proton transport and dynamics in membrane proteins for the prediction and analysis. In this model, the proton of primary interest is described quantum mechanically because of its unique traits, while other mobile ions and the environment are treated in a classical sense. Additionally, the membrane protein plays an essential role in the permeation process so it is modeled explicitly, whereas a dielectric continuum treatment of solvent medium promises a reasonable approximation to numerous solvent molecules. These multiscale and multiphysics treatments are coupled by the adaptive solvent-solute interface. During the permeation process the protons are under intensive interactions, which include long range or Coulomb interactions and short-range interactions. Previous work focuses mainly on the electrostatics interaction while the present work provides a more quantitative description of the short-range generalized correlation.

In the present approach, the generalized correlation is specifically split as proton-proton, proton-ion, proton-water, and proton-protein interactions, which are formulated as convolutions of interaction kernels and particle number densities. Number densities of mobile ionic species, including proton and all other ions, follow the same definitions and treatments as in our original model.[16,17] The number density of water can be either approximated as a constant or Gaussian function depends on different sizes of channel pores. In contrast, the density of channel protein atoms is accounted explicitly and a multiscale discrete-continuum proton-protein interaction is considered. Upon physical characteristics, interaction kernels are designed in a uniform formulation with appropriate parameters to reflect biological properties of ion species and specific mathematical properties. Based on these treatments, the generalized correlation is able to include the ion-ion short-range interactions such as van der Waals interaction and finite size effect. More importantly, it is well known that extremely narrow channel pore will induce geometrical confinement to the freedom of water motion. As such, the interaction between ion and water is significantly different there from that of the bulk region. A well designed generalized correlation can capture this difference successfully. In this work, the generalized correlation has a more quantitative description which balances biological details and simulation efficiency, and thus it is a reliable complement to the electrostatic potential in the total Hamiltonian of protons.

Several advanced numerical algorithms are equipped to handle mathematical challenges in solving the coupled governing equations. The original generalized Laplace-Beltrami equation is solved through a parabolic equation with pseudo time and the Laplace-Beltrami potential is converted to a density related expression in order to avoid the direct evaluation of the proton wavefunctions.[17] The DNM method and the MIB method are utilized to handle singular charges and discontinuous coefficients in the generalized Poisson-Boltzmann equation. Based on the generalized Kohn-Sham equation, formulations are derived for the proton number density and probability current. Finally, a surface driven self-consistent iteration is employed to solve three coupled governing equations.

Validation of the proposed model and performance of the related numerical techniques are verified by simulations with the popular Gramicidin A (GA) channel protein. First, as a component of GC, the proton-water interaction is specifically tested with various simplified channel parameters to demonstrate the geometric confinement effect. Then the realistic generalized correlation is calculated and mapped on the GA surface to compare with the result of electrostatic potential. Furthermore, each component of the generalized correlation is visualized to give a detailed physical illustration and the combination of generalized correlation and electrostatics is displayed to explain the GA selectivity. Finally, current voltage (I-V) curves and conductance-concentration curves, which represent proton transport properties, are investigated over a large number of combinations of applied voltages and reference bulk concentrations. The good agreement

of our model predictions against experimental data validates the present QDC with generalized correlation model.

ACKNOWLEDGMENTS

This work was supported in part by National Science Foundation (NSF) Grant No. CCF-0936830, National of Institutes of Health (NIH) Grant No. R01GM-090208 and MSU Competitive Discretionary Funding Program Grant No. 91-4600.

[1]C. D. Cole, A. S. Frost, N. Thompson, M. Cotten, T. A. Cross, and D. D. Busath, "Noncontact dipole effects on channel permeation. VI. 5F- and 6F-Trp Gramicidin channel currents," Biophys. J. **83**, 1974–1986 (2002).
[2]S. Cukierman, E. P. Quigley, and D. S. Crumrine, "Proton conduction in Gramicidin A and in its dioxolane-linked dimer in different lipid bilayers," Biophys. J. **73**, 2489–2502 (1997).
[3]G. Eisenman, B. Enos, J. Hagglund, and J. Sandbloom, "Gramicidin as an example of a single-filing ion channel," Ann. N.Y. Acad. Sci. **339**, 8 (1980).
[4]B. Roux, T. Allen, S. Berneche, and W. Im, "Theoretical and computational models of biological ion channels," Q. Rev. Biophys. **37**(1), 15–103 (2004).
[5]S.-H. Chung and S. Kuyucak, "Recent advances in ion channel research," Biochim. Biophys. Acta **1565**, 267–286 (2002).
[6]M. B. Partenskii, V. Dormann, and P. C. Jordan, "Influence of a channel-forming peptide on energy barriers to ion permeation, viewed from a continuum dielectric perspective," Biophys. J. **67**, 1429–1438 (2002).
[7]B. Corry, S. Kuyucak, and S.-H. Chung, *Test of Poisson-Nernst-Planck Theory in Ion Channels* (The Rockefeller University Press, 1999), Vol. 114, pp. 597–599.
[8]L. I. Krishtalik, "The mechanism of the proton transfer: An outline," Biochim. Biophys. Acta **1458**, 6–27 (2000).
[9]U. Hollerbach, D. Chen, and B. S. Eisenberg, "Two- and three-dimensional Poisson-Nernst-Planck simulations of current flow through Gramicidin A," J. Sci. Comput. **16**, 373–409 (2002).
[10]A. B. Mamonov, R. D. Coalson, A. Nitzan, and M. G. Kurnikova, "The role of the dielectric barrier in narrow biological channels: A novel composite approach to modeling single-channel currents," Biophys. J. **84**, 3646–3661 (2003).
[11]W. Dyrka, A. T. Augousti, and M. Kotulska, "Ion flux through membrane channels: An enhanced algorithm for the Poisson-Nernst-Planck model," J. Comput. Chem. **29**, 1876–1888 (2008).
[12]A. E. Cardenas, R. D. Coalson, and M. G. Kurnikova, "Three-dimensional Poisson-Nernst-Planck theory studies: Influence of membrane electrostatics on Gramicidin A channel conductance," Biophys. J. **79**, 80–93 (2000).
[13]Q. Zheng, D. Chen, and G. W. Wei, "Second-order Poisson-Nernst-Planck solver for ion transport," J. Comput. Phys. **230**, 5239–5262 (2011).
[14]M. F. Schumaker, R. Pomes, and B. Roux, "A combined molecular dynamics and diffusion model of single proton conduction through gramicidin," Biophys. J. **79**, 2840–2857 (2000).
[15]S. Kuyucak, O. S. Andersen, and S.-H. Chung, "Models of permeation in ion channels," Rep. Prog. Phys. **64**, 1427–1472 (2001).
[16]D. Chen and G. W. Wei, "Quantum dynamics in continuum for proton transport I: Basic formulation," Comm. Comp. Phys. (in press).
[17]D. Chen, Z. Chen, and G. W. Wei, "Quantum dynamics in continuum for proton transport II: Variational solvent-solute intersurface," Int. J. Numer. Meth. Biomed. Eng. **28**, 25–51 (2012).
[18]Q. Zheng and G. W. Wei, "Poisson-Boltzmann-Nernst-Planck model," J. Chem. Phys. **134**, 194101 (2011).
[19]G. W. Wei, Q. Zheng, Z. Chen, and K. Xia, "Differential geometry based ion transport models," SIAM Rev. (in press).
[20]A. Singer, D. Gillespie, J. Norbury, and R. S. Eisenberg, "Singular perturbation analysis of the steady state Poisson-Nernst-Planck system: Applications to ion channels," Eur. J. Appl. Math. **19**, 541–560 (2008).
[21]M. Burger, B. S. Eisenberg, and E. Heinz, "Inverse problems related to ion channel selectivity," SIAM J. Appl. Math. **67**(4), 960–989 (2002).
[22]B. S. Eisenberg and W. S. Liu, "Poisson-Nernst-Planck systems for ion channels with permanent charges," SIAM, J. Math. Anal. **38**(6), 1932–1966 (2006).
[23]G. W. Wei, "Differential geometry based multiscale models," Bull. Math. Biol. **72**, 1562–1622 (2010).
[24]J. F. Nagle and H. J. Morowitz, "Molecular mechanisms for proton transport in membranes," Proc. Natl. Acad. Sci. U.S.A. **1458**(72), 298–302 (1978).
[25]D. A. Perlman, D. A. Case, J. W. Caldwell, W. S. Ross, T. E. Cheatham, S. Debolt, D. Ferguson, G. Seibel, and P. Kollman, "Amber, a package of computer programs for applying molecular mechanics, normal mode analysis, molecular dynamics and free energy calculations to simulate the structural and energetic properties of molecules," Comput. Phys. Commun. **91**, 1–41 (1995).
[26]A. D. MacKerell, Jr., D. Bashford, M. Bellot, R. L. Dunbrack, Jr., J. D. Evanseck, M. J. Field, S. Fischer, J. Gao, H. Guo, S. Ha, D. Joseph-McCarthy, L. Kuchnir, K. Kuczera, F. T. K. Lau, C. Mattos, S. Michnick, T. Ngo, D. T. Nguyen, B. Prodhom, W. E. Reiher III, B. Roux, M. Schlenkrich, J. C. Smith, R. Stote, J. Straub, M. Watanabe, J. Wiorkiewicz-Kuczera, D. Yin, and M. Karplus, "All-atom empirical potential for molecular modeling and dynamics studies of proteins," J. Phys. Chem. B **102**(18), 3586–3616 (1998).
[27]W. F. van Gunsteren, S. Billeter, A. A. Eising, P. H. Hunenberger, P. Kruger, A. E. Mark, W. R. P. Scott, and I. G. Tironi, "*Biomolecular Simulation: The GROMOS96 Manual and User Guide*" (vdf Hochschulverlag AG an der ETH zurich and BIOMOS b.v.: Zurich, Groningen, 1996).
[28]R. Pomes and B. Roux, "Molecular mechanism of H^+ conduction in the single-file water chain of the gramicidin channel," Biophys. J. **82**, 2304–2316 (2002).
[29]S. Edwards, B. Corry, S. Kuyucak, and S.-H. Chung, "Continuum electrostatics fails to describe ion permeation in the gramicidin channel," Biophys. J. **83**, 1348–1360 (2002).
[30]E. Alexov and M. R. Gunner, "Calculated protein and proton motions coupled to electron transfer: Electron transfer from Q_A^- to Q_B in bacterial photosynthetic reaction centers," Biochemistry **38**, 8253–8270 (1999).
[31]R. I. Cukier, "Theory and simulation of proton-coupled electron transfer, hydrogen-atom transfer, and proton translocation in proteins," Biochim. Biophys. Acta **1655**, 37–44 (2004).
[32]L. M. S. Shepherd and C. A. Morrison, "Simulating proton transport through a simplified model for trans-membrane proteins," J. Phys. Chem. **114**, 7047–7055 (2010).
[33]R. Pomes and B. Roux, "Theoretical study of H^+ translocation along a model proton wire," J. Phys. Chem. **100**, 2519–2527 (1996).
[34]R. Pomes and B. Roux, "Structure and dynamics of a proton wire: A theoretical study of H^+ translocation along the single-file water chain in the Gramicidin A channel," Biophys. J. **71**, 19–39 (2002).
[35]U. W. Schmitt and G. A. Voth, "The computer simulation of proton transport in water," J. Chem. Phys. **111**, 9361–9381 (1999).
[36]T. Decoursey, "Voltage-gated proton channels and other proton transfer pathways," Physiol. Rev. **83**, 475–579 (2003).
[37]J. Bothma, J. Gilmore, and R. McKenzie, "The role of quantum effects in proton transfer reactions in enzymes: Quantum tunneling in a noisy environment?," New J. Phys. **12**, 055002 (2010).
[38]K. Drukker, S. H. de Leeuw, and H. Hammes-Schiffer, "Proton transport along water chains in an electric field," J. Chem. Phys. **108**, 6799–6808 (1998).
[39]H. Decornez, K. Drukker, and H. Hammes-Schiffer, "Solvation and hydrogen-bonding effects on proton wires," J. Phys. Chem. A **103**, 2891–2898 (1999).
[40]S. H. Yan, L. Liang Zhang, R. I. Cukier, and Y. X. Bu, "Exploration on regulating factors for proton transfer along hydrogen-bonded water chains," ChemPhysChem **8**, 944–954 (2007).
[41]R. I. Cukier, "Quantum molecular dynamics simulation of proton transfer in cytochrome c oxidase," Biochim. Biophys. Acta **1656**, 189–202 (2004).
[42]M. L. Wang, Z. Y. Lu, and W. T. Yang, "Nuclear quantum effects on an enzyme-catalyzed reaction with reaction path potential: Proton transfer in triosephosphate isomerase," J. Chem. Phys. **124**, 124516 (2006).
[43]Y. C. Zhou, S. Zhao, M. Feig, and G. W. Wei, "High order matched interface and boundary method for elliptic equations with discontinuous coefficients and singular sources," J. Comput. Phys. **213**(1), 1–30 (2006).
[44]S. N. Yu, W. H. Geng, and G. W. Wei, "Treatment of geometric singularities in implicit solvent models," J. Chem. Phys. **126**, 244108 (2007).
[45]W. Geng, S. Yu, and G. W. Wei, "Treatment of charge singularities in implicit solvent models," J. Chem. Phys. **127**, 114106 (2007).
[46]D. Chen, Z. Chen, C. Chen, W. H. Geng, and G. W. Wei, "MIBPB: A software package for electrostatic analysis," J. Comput. Chem. **32**, 756–770 (2011).

[47]Y. Hyon, B. Eisenberg, and C. Liu, "A mathematical model of the hard sphere repulsion in ionic solutions," Commun. Math. Sci. **9**, 459–475 (2011).
[48]S. Zhou, Z. Wang, and B. Li, "Mean-field description of ionic size effects with non-uniform ionic sizes: A numerical approach," Phys. Rev. E **84**, 021901 (2011).
[49]S. Braun-Sand, A. Burykin, Z. T. Chu, and A. Warshel, "Realistic simulations of proton transport along the gramicidin channel: Demonstrating the importance of solvation effects," J. Phys. Chem. B **109**, 583–592 (2005).
[50]S. Billeter and W. van Gunsteren, "A modular molecular dynamics/quantum dynamics program for non-adiabatic proton transfers in solution," Comput. Phys. Commun. **107**, 61–91 (1997).
[51]S. Billeter and W. van Gunsteren, "Protonizable Water Model for Quantum Dynamical Simulations," J. Phys. Chem. **102**, 4669–4678 (1998).
[52]R. F. Snider, G. W. Wei, and J. G. Muga, "Moderately dense gas quantum kinetic theory: Transport coefficient expressions," J. Chem. Phys. **105**, 3066–3078 (1996).
[53]R. F. Snider, G. W. Wei, and J. G. Muga, "Moderately dense gas quantum kinetic theory: Aspects of pair correlations," J. Chem. Phys. **105**, 3057–3065 (1996).
[54]Z. Chen, N. A. Baker, and G. W. Wei, "Differential geometry based solvation models II: Lagrangian formulation," J. Math. Biol. **63**, 1139–1200 (2011).
[55]D. Chen and G. W. Wei, "Modeling and simulation of electronic structure, material interface and random doping in nano-electronic devices," J. Comput. Phys. **229**, 4431–4460 (2010).
[56]A. A. Kornyshev, A. M. Kuznetsov, E. Spohr, and J. Ulstrup, "Kinetics of proton transport in water," J. Phys. Chem. B **107**, 3351–3366 (2003).
[57]T. J. F. Day, A. V. Soudackov, M. Cuma, U. W. Schmitt, and G. A. Voth, "A second generation multistate empirical valence bond model for proton transport in aqueous systems," J. Chem. Phys. **117**, 5840–5849 (2002).
[58]Z. Chen, N. A. Baker, and G. W. Wei, "Differential geometry based solvation models I: Eulerian formulation," J. Comput. Phys. **229**, 8231–8258 (2010).
[59]P. W. Bates, Z. Chen, Y. H. Sun, G. W. Wei, and S. Zhao, "Geometric and potential driving formation and evolution of biomolecular surfaces," J. Math. Biol. **59**, 193–231 (2009).
[60]G. W. Wei, Y. H. Sun, Y. C. Zhou, and M. Feig, "Molecular multiresolution surfaces," 1–11 (2005); e-print arXiv:math-ph/0511001v1.
[61]P. W. Bates, G. W. Wei, and S. Zhao, "Minimal molecular surfaces and their applications," J. Comput. Chem. **29**(3), 380–91 (2008).
[62]L.-T. Cheng, Y. Xie, J. Dzubiella, J. A. McCammon, J. Che, and B. Li, "Coupling the level-set method with molecular mechanics for variational implicit solvation of nonpolar molecules," J. Chem. Theory Comput. **5**, 257–266 (2009).
[63]T. J. Dolinsky, J. E. Nielsen, J. A. McCammon, and N. A. Baker, "PDB2PQR: An automated pipeline for the setup, execution, and analysis of Poisson-Boltzmann electrostatics calculations," Nucleic Acids Res. **32**, W665–W667 (2004).
[64]T. Urbic, V. Vlachy, and K. Dill, "Confined water: A Mercedes-Benz model study," J. Phys. Chem. **110**, 4963–4970 (2006).